

# Generative Adversarial Networks: A Survey and Taxonomy

Zhengwei Wang, Qi She, Tomás E. Ward

## Abstract—

Generative adversarial networks (GANs) have been extensively studied in the past few years. Arguably the revolutionary techniques are in the area of computer vision such as plausible image generation, image to image translation, facial attribute manipulation and similar domains. Despite the significant success achieved in computer vision field, applying GANs over real-world problems still have three main challenges: (1) High quality image generation; (2) Diverse image generation; and (3) Stable training. Considering numerous GAN-related research in the literature, we provide a study on the architecture-variants and loss-variants, which are proposed to handle these three challenges from two perspectives. We propose loss and architecture-variants for classifying most popular GANs, and discuss the potential improvements with focusing on these two aspects. While several reviews for GANs have been presented, there is no work focusing on the review of GAN-variants based on handling challenges mentioned above. In this paper, we review and critically discuss 7 architecture-variant GANs and 9 loss-variant GANs for remedying those three challenges. The objective of this review is to provide an insight on the footprint that current GANs research focuses on the performance improvement. Code related to GAN-variants studied in this work is summarized on [https://github.com/sheqi/GAN\\_Review](https://github.com/sheqi/GAN_Review).

**Index Terms**—Generative Adversarial Networks, Computer Vision, Architecture-variants, Loss-variants, Stable Training.



## 1 INTRODUCTION

GENERATIVE adversarial networks (GANs) are attracting growing interests in the deep learning community [1]–[6]. GANs have been applied to various domains such as computer vision [7]–[14], natural language processing [15]–[18], time series synthesis [19]–[22], semantic segmentation [23]–[27] etc. GANs belong to the family of generative model. Comparing to other generative models e.g., variational autoencoders, GANs favor advantages such as handling sharp estimated density functions, efficiently generating desired samples, eliminating deterministic bias and good compatibility with the internal neural architecture. These properties enable GANs achieve success especially in the computer vision field e.g., plausible image generation [28]–[32], image to image translation [2], [33]–[39], image super-resolution [25], [40]–[43] and image completion [44]–[48].

However, GANs suffer challenges from two aspects: (1) Hard to train — It is non-trivial for discriminator and generator to achieve Nash equilibrium during the training and the generator cannot learn the distribution of the full datasets well, which is known as mode collapse. Lots of work has been carried out in this area [49]–[52]; and (2) Hard to evaluate — the evaluation of GANs can be considered as an effort to measure the dissimilarity between real distribution  $p_r$  and generated distribution  $p_g$ . Unfortunately, the accurate estimation of  $p_r$  is intractable. Thus, it is challenging to have a good estimation of the correspondence between  $p_r$  and  $p_g$ . Previous work has introduced evaluation metrics

for GANs [53]–[61]. The first aspect have effect on the performance for GANs directly e.g., image quality, image diversity and stable training. In this work. we are going to study the existing GAN-variants that handle the first aspect in the area of computer vision while the second one can refer to the work [53], [61].

Current GANs research focuses on two directions: (1) Improve the training for GANs; and (2) Apply GANs to realize real-world applications. First research direction aims to improve the performance for GANs and it is the footstone for the second aspect. Considering numerous research work in the literature, we give a brief review on the GAN-variants that focus on the training scenery in this study. The improvement of the training process can have benefits to the performance of GANs as follows: (1) Generated image diversity (also known as mode diversity); (2) Generated image quality; and (3) Stable training such as remedying the vanishing gradient for generator. In order to improve the performance as mentioned above, modification for GANs can be done from either architecture side or loss side. We will study the GAN-variants coming from both sides that improve the performance for GANs. Rest of the paper is organized as follows: (1) We introduce the search strategy and part of the results (complete results are illustrated in Supplementary material) for the existing GANs papers in the area of computer vision; (2) We introduce the related review work for GANs and illustrate the difference from those reviews to this work; (3) We give a brief introduction on GANs; (4) We review the architecture-variant GANs in the literature; (5) We review the loss-variant GANs in the literature; (6) We summarize the GAN-variants in this study and illustrate their difference and relationship; and (7) We conclude this review and prospect the future work for GANs.

Zhengwei Wang and Tomás E. Ward are with Insight Centre for Data Analytics, Dublin City University, Dublin, Ireland. e-mail: zhengwei.wang22@mail.dcu.ie, tomas.ward@dcu.ie  
Qi She is with Intel Labs, Beijing, China. e-mail: qi.she@intel.com

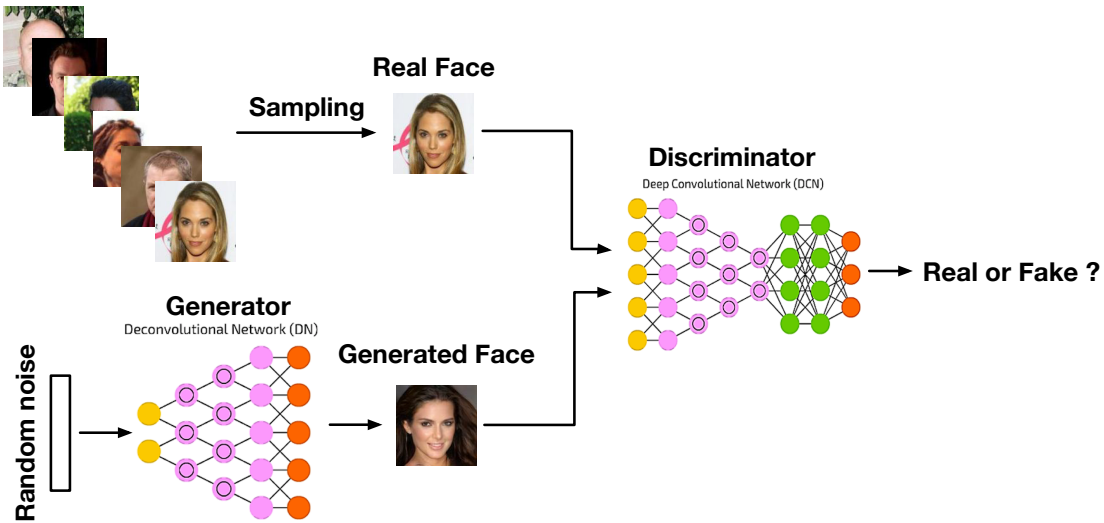


Fig. 1. Architecture of a GAN. Two deep neural networks (discriminator ( $D$ ) and generator ( $G$ )) are synchronously trained during the learning stage. Discriminator is optimized in order to distinguish between real images and generated images while generator is trained for the sake of fooling discriminator from discerning between real images and generated images.

## 2 SEARCH STRATEGY AND RESULTS

A review of the literature was performed to identify research work describing GANs. Papers first were identified through manual search of the online datasets (Google Scholar and IEEE Xplore) by using keyword “generative adversarial networks”. Secondly papers related to computer vision were manually selected. This search ended up on 17th May 2019.

A total of 322 papers describing GANs related to computer vision were identified. The earliest paper was in 2014 [1]. Papers were classified into three categories regarding their repository, namely conference, arXiv and journal. More than half of papers were presented at conferences (204, 63.3%). The rest were journal articles (58, 18.0%) and arXiv pre-prints (60, 18.6%). Details of statistics and paper list are described in Supplementary material.

## 3 RELATED WORK

Some reviews on GANs have been carried out in the literature. A comparison based on the performance has been done for different GANs in [62]. It focuses on the experimental validation across different types of GANs benchmarking on LSUN-BEDROOM [63], CELEBA-HQ-128 [64] and CIFAR10 [65] image datasets. Results suggest that the original GAN [1] with spectral normalization [66] as the default choice when applying GANs to a new dataset. A limitation of this work is that benchmark datasets do not consider much diversity. Thus the benchmark results tend to focus more on evaluation of the image quality, which may ignore the GAN’s efficacy that produces diverse images. Work [67] surveys the different GAN architectures and their evaluation metrics. A further comparison on different architecture-variants’ performance, applications, complexity and so on, needs to be explored. Papers [68]–[70] focus on the investigation of the development trends and the applications of GANs. They compare GAN-variants through different applications. Comparing this review to the current literature, this review introduces GAN-variants based on their

performance including producing high quality and diverse images, stable training, ability of handling the vanishing gradient etc.. from architecture basis and loss function basis. This work also provides the comparison between GAN-variants presented in this paper.

## 4 GENERATIVE ADVERSARIAL NETWORKS

Figure. 1 demonstrates the architecture of a typical GAN. The architecture comprises two components that one is discriminator ( $D$ ) distinguishing between real images and generated images while the other one is generator ( $G$ ) generating the images that fool the discriminator. Given a distribution  $\mathbf{z} \sim p_{\mathbf{z}}$ ,  $G$  defines a probability distribution  $p_g$  as the distribution of the samples  $G(\mathbf{z})$ . The objective of a GAN is to learn the generator’s distribution  $p_g$  that approximates the real data distribution  $p_r$ . Optimization of a GAN is performed with respect to a joint loss for  $D$  and  $G$

$$\min_G \max_D \mathbb{E}_{\mathbf{x} \sim p_r} \log[D(\mathbf{x})] + \mathbb{E}_{\mathbf{z} \sim p_{\mathbf{z}}} \log[1 - D(G(\mathbf{z}))]. \quad (1)$$

GANs, as a member of deep generative model (DGM) family, has attracted exponentially growing interest in the deep learning community because of some advantages comparing to the tradition DGMs: (1) GANs are able to produce better samples than other DGMs. Comparing to the most well-known DGMs—variational autoencoder (VAE), GANs are able to produce any type of probability density while VAE is not able to generate sharp images; (2) The GAN framework can train any type of generator network. Other DGMs may have pre-requirements for the generator e.g., output layer of generator is Gaussian; (3) There is no restriction on the size of the latent variable etc.. These advantages make GANs achieve the state of art performance on producing synthetic data especially for image data.

Lots of GAN-variants have been proposed in the literature to improve the performance for GANs. GAN-variants can be divided into two types: (1) Architecture-variants.

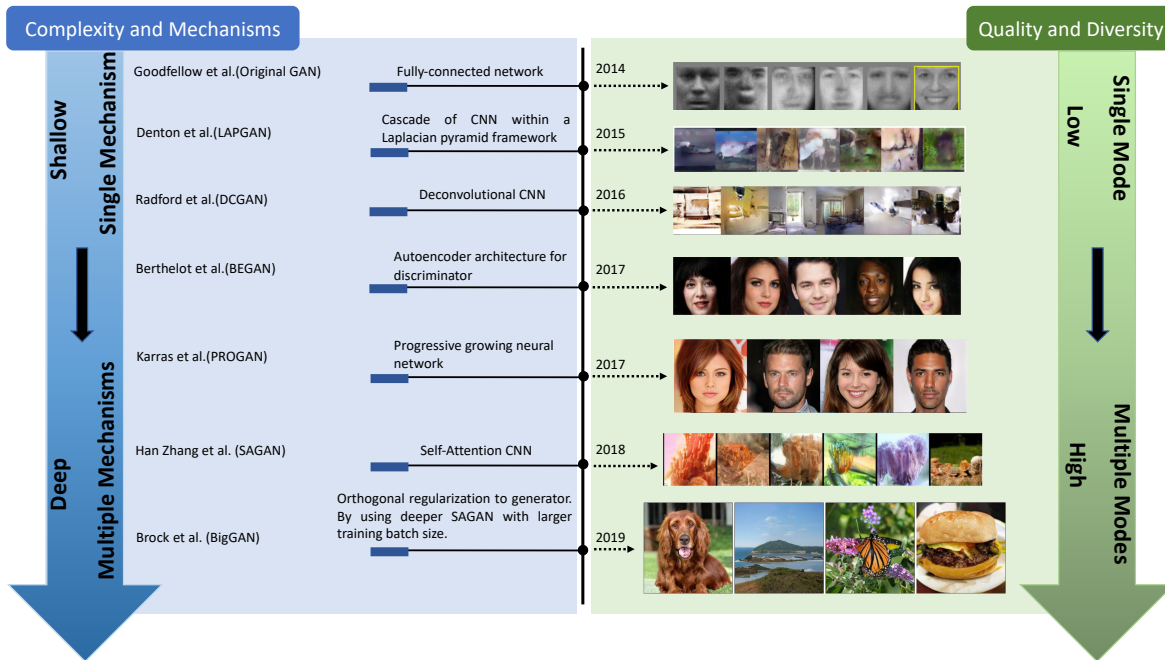


Fig. 2. Timeline of architecture-variant GANs. Complexity in blue stream refers to size of the architecture and computational cost such as batch size. Mechanisms refer to number of types of models used in the architecture (e.g., BEGAN uses autoencoder architecture for discriminator while a deconvolutional neural network is used for generator. In this case, two mechanisms are used).

The first proposed GAN used fully connected neural networks [1] so specific type of architecture may be beneficial to specific application e.g., convolutional neural network for images and recurrent neural network for time series data; and (2) Loss-variants. Revise the loss function in equation (1) to enable more stable learning for  $G$ .

## 5 ARCHITECTURE-VARIANT GANS

There are many types of architecture-variants have been proposed in the literature (see Fig.2) [32], [33], [71]–[73]. Architecture-variant GANs are mainly proposed for the purpose of different applications e.g., image to image transfer [33], image super resolution [40], image completion [74], and generating text to images [75]. In this section, we provide the review on architecture-variants that helps improve the performance for GANs from three aspects mentioned before. Review for those architecture-variant for different applications can be referred to work [67], [69].

### 5.1 Fully-connected GAN (FCGAN)

The original GAN paper [1] uses fully-connected neural networks for both generator and discriminator. This architecture-variant is applied for some simple image datasets i.e., MNIST [76], CIFAR-10 [65] and Toronto Face Dataset. It does not have good generalization for more complex images.

### 5.2 Laplacian Pyramid of Adversarial Networks (LAPGAN)

LAPGAN is proposed for producing higher resolution images comparing to the original GAN [77]. Figure. 3 demonstrates the up-sampling process of generator in LAPGAN

from right to left. LAPGAN utilizes a cascade of CNN within a Laplacian pyramid framework [79] to generate high quality images.

### 5.3 Deep Convolutional GAN (DCGAN)

DCGAN is the first work that applies deconvolutional neural networks architecture for  $G$  [71]. Figure. 4 illustrates the proposed architecture for  $G$ . Deconvolution is proposed to visualize the features for convolutional neural network (CNN) and has shown the good performance for CNN visualization [80]. DCGAN deploys the spatial up-sampling ability of the deconvolution operation for  $G$ , which enables the generation of higher resolution images using GANs.

### 5.4 Boundary Equilibrium GAN (BEGAN)

BEGAN uses an autoencoder architecture for discriminator which is first proposed in EBGAN [81] (see Fig. 5). Comparing to traditional optimization, BEGAN matches autoencoder loss distributions using a loss derived from the Wasserstein distance instead of match data distributions directly. This modification helps  $G$  able to generate easy-to-reconstruct data for the autoencoder at the beginning because generated data is close to 0 and the real data distribution has not been learned accurately yet, which prevents that  $D$  easily win  $G$  at the early training stage as mentioned before.

### 5.5 Progressive GAN (PROGAN)

PROGAN is a revolutionary architecture-variant which proposes progressive steps toward the performance of GANs [73]. This architecture uses the idea of progressive neural networks that is first proposed in [82]. This technology are immune to forgetting and can leverage prior

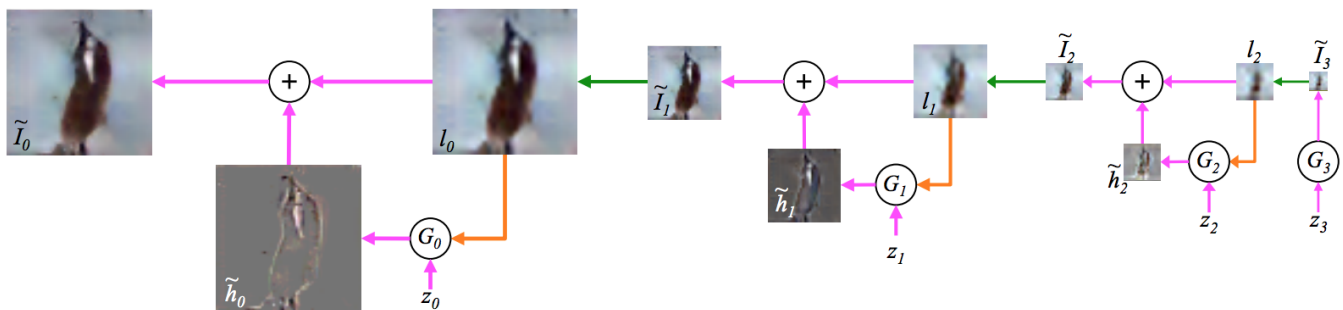


Fig. 3. Up-sampling process of generator in LAPGAN (from right to left). The up-sampling process is marked using green arrow and conditioning process via CGAN [78] is marked using orange arrow. The process starts to use  $G_3$  to generate image  $\tilde{I}_3$  and then up-sample the image  $\tilde{I}_3$  to  $l_2$ . Together with another noise  $z_2$ ,  $G_2$  generates a difference image  $\tilde{h}_2$  and add  $\tilde{h}_2$  to  $l_2$  to be the generated image  $\tilde{I}_2$ . The rest can be done in the same manner. LAPGAN contains 3 generators in this work in order to up-sample the image. Figure from [77].

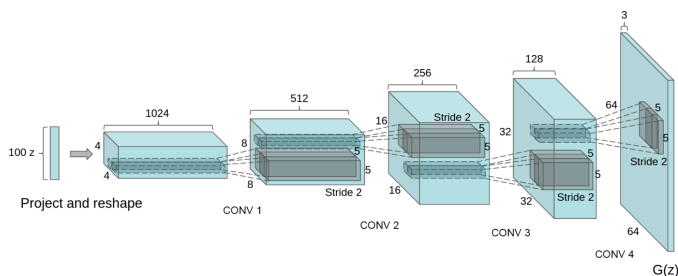


Fig. 4. Detail of DCGAN architecture for generator. This generator successfully generates  $64 \times 64$  pixel image for LSUN scene dataset, which is more complex than the datasets used in the original work. Figure from [71].

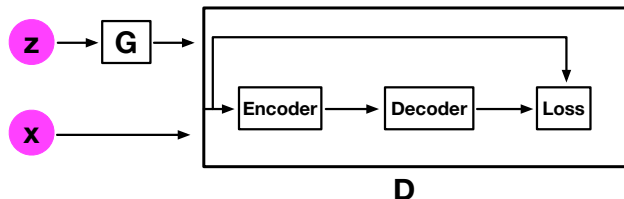


Fig. 5. Illustration of BEGAN architecture.  $z$  is the latent variable for  $G$  and  $x$  is input image. BEGAN deploys autoencoder architecture for the discriminator. Loss is calculated using  $L_1$  or  $L_2$  norm at pixel level.

knowledge via lateral connections to previously learned features, which is widely applied for learning complex sequences of tasks. Figure. 6 demonstrates the training process for PROGAN. Training starts with low resolution  $4 \times 4$  pixels image. Both  $G$  and  $D$  start to grow with the training progressing. Importantly, all variables remain trainable through this growing process. This progressive training strategy enables substantially more stable learning for both two networks. By increasing the resolution little by little, the networks are continuously asked a much simpler question comparing to the end goal of discovering a mapping from latent vectors. Current state-of-art GANs all deploy this type of training strategy and have produced impressive plausible images [28], [73], [83].

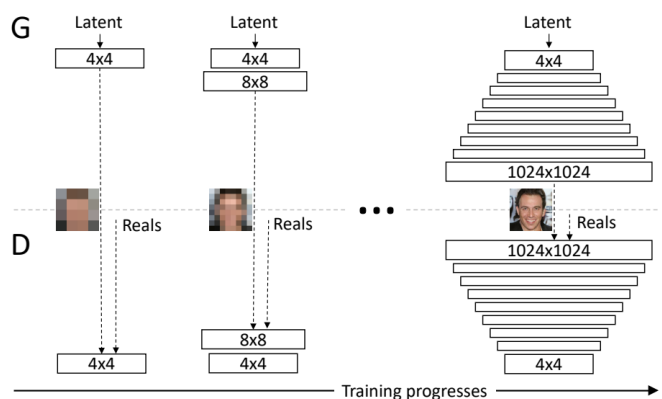


Fig. 6. Progressive growing step for PROGAN during the training process. Training starts with  $4 \times 4$  pixels image resolution. With the training step growing, layers are incrementally added to  $G$  and  $D$  which increases the resolution for the generated images. All existing layers are trainable throughout the training stage. Figure from [73].

## 5.6 Self-attention GAN (SAGAN)

Traditional CNN can only capture the local spatial information and the receptive field may not cover enough structure, which causes CNN-based GAN has difficulty in learning multi-class image datasets e.g., Imagenet and the key components in generated images may shift and the nose in a generated image does not appear in right position. Self-attention mechanism has been proposed to keep large receptive field and keeps computational efficiency for CNN [84]. SAGAN deploys the self-attention mechanism to design the architectures of discriminator and generator for GANs [85] (see Fig. 7). Benefit from the self-attention mechanism, SAGAN is able to learn global, long-range dependencies for generating the images. It has achieved great performance on the multi-class image generation based on the Imagenet datasets.

## 5.7 BigGAN

BigGAN [83] has achieved the state-of-the-art performance on the Imagenet datasets. It is designed based on the SAGAN. This work demonstrates that the increase of batch

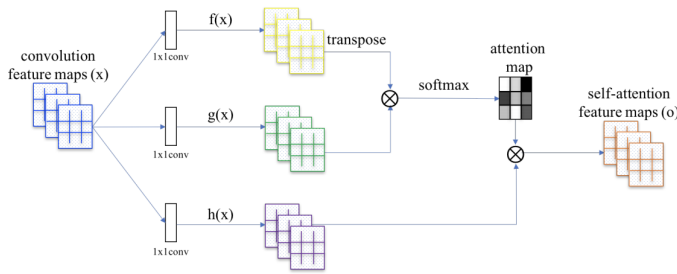


Fig. 7. Self-attention mechanism architecture proposed in the paper.  $f$ ,  $g$  and  $h$  are corresponding to query, key and value in the self-attention mechanism. The attention map indicates the long-range spatial dependencies. The  $\otimes$  is matrix multiplication. Figure from [85].

size and the model complexity for complex image datasets can dramatically improve the performance for GANs.

## 5.8 Summary

We have provided an overview of architecture-variant GANs in the literature, which aims to improve the performance for GANs based on three challenges: (1) Image quality; (2) Mode diversity; and (3) Vanishing gradient. Summary for the architecture-variant can be seen in Fig. 8. All

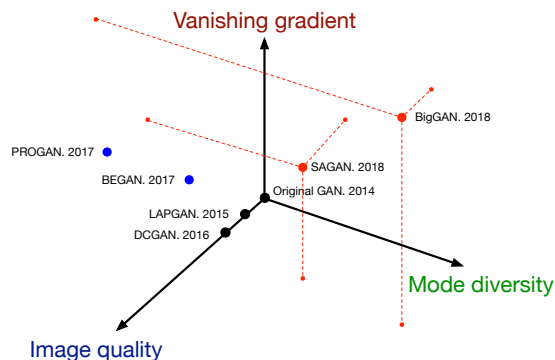


Fig. 8. Summary of recent architecture-variant GANs for solving the three challenges. The challenges are categorized by three orthogonal axes. Larger value for each axis indicates better performance. Red points indicate the GAN-variant covers all three challenge, blue points cover two, and black points cover only one challenge.

proposed architecture-variants are able to improve the image quality. SAGAN is proposed for improving the capacity of multiclass learning for GANs, which is to produce more diverse images. Benefit from the architecture in SAGAN, BigGAN is designed for improving both image quality and image diversity. It should be noted that both PROGAN and BigGAN are able to produce high resolution images. BigGAN realizes the high resolution by increasing the batch size and author mention that progressive growing [73] operation is unnecessary when batch size is large enough (2048 used in the original paper [83]). However, progressive growing operation is still needed when GPU memory is limited (large batch size is hungry for the GPU memory). Benefiting from the spectrum normalization (SN), which will be discussed in loss-variant GAN part, both SAGAN and BigGAN is effective for the vanishing gradient. These milestone architecture-variants indicate a strong advantage

of GAN — compatibility, where a GAN is open to any type of neural architecture. This property enables GANs been applied to lots of different applications.

Regarding the improvements achieved by different architecture-variant GANs, we are going to give an analysis on the interconnections and comparisons of the architecture-variants presented in this study. Back to the FCGAN stated in the original GAN, this architecture-variant can only generate simple image datasets. Such a limitation is caused by the network architecture, where the capacity of FC networks is very limited. Research work for improving the performance of GANs starts from designing more complex architectures for GANs. A more complex image datasets (e.g., ImageNet) have higher resolution and diversity comparing to simple image datasets (e.g., MNIST).

In the context of producing higher resolution images, it can be easily came up with increasing the size of generator intuitively. LAPGAN and DCGAN up-sample the generator from this perspective. Benefit from the concise deconvolutional up-sampling process and easy generalization of DCGAN, the architecture in DCGAN is more widely used in the GANs literature. It should be noticed that most of GANs in the computer vision area use the deconvolutional neural network as the generator, which is first used in DCGAN. Therefore, DCGAN is one of classical GAN-variants in the literature.

Ability of producing high quality images is important index. This can be improved by designing architecture as well. BEGAN and PROGAN demonstrate approaches from this perspective. With the same architecture used for generator in DCGAN, BEGAN redesigns discriminator by including encoder and decoder, where discriminator tries to distinguish the difference of generated images and autoencoded images in the pixel space. Image quality has been improved in this case. Based on DCGAN, PROGAN demonstrates a progressive approach that incrementally train a DCGAN-similar architecture. This novel progress cannot only improve the image quality but also produce higher resolution images.

Producing diverse images is the most challenging task for GANs and it is very difficult for GANs to successfully produce images based on ImageNet before. It is difficult for traditional CNNs to learn global and long-range dependencies from images. Thanks to self-attention mechanism, SAGAN integrates self-mechanism to both discriminator and generator, which help GANs a lot in terms of learning multi-class images. Moreover, BigGAN, based on foundation of SAGAN, introduces a deeper GAN architecture with humongous batch size, which produces high quality and diverse images in the ImageNet and is the current state-of-the-art.

## 6 LOSS-VARIANT GANs

Loss-variant of GANs is developed by changing the loss function in equation (1). Even the original work [1] has already proved the global optimality and the convergence of training a GAN, but it still states the unstable problem for training a GAN. The problem is caused by the global optimality which is stated in [1]. The global optimality is given when an optimal  $D$  is achieved for any  $G$ . So the

optimal  $D$  is achieved when the derivative  $D$  for the loss in equation (1) equals to 0. So we have

$$\begin{aligned} -\frac{p_r(\mathbf{x})}{D(\mathbf{x})} + \frac{p_g(\mathbf{x})}{1-D(\mathbf{x})} &= 0, \\ D^*(\mathbf{x}) &= \frac{p_r(\mathbf{x})}{p_r(\mathbf{x}) + p_g(\mathbf{x})}, \end{aligned} \quad (2)$$

where  $\mathbf{x}$  is real data,  $D^*(\mathbf{x})$  is the optimal discriminator,  $p_r(\mathbf{x})$  is real data distribution and  $p_g(\mathbf{x})$  is generated data distribution over real data  $\mathbf{x}$ . We have got the optimal discriminator  $D$  so far. When we have the optimal  $D$ , the loss for  $G$  can be visualized by substituting  $D^*(\mathbf{x})$  into equation (1)

$$\begin{aligned} \mathcal{L}_G &= \mathbb{E}_{\mathbf{x} \sim p_r} \log \frac{p_r(\mathbf{x})}{\frac{1}{2}[p_r(\mathbf{x}) + p_g(\mathbf{x})]} + \\ &\quad \mathbb{E}_{\mathbf{x} \sim p_g} \log \frac{p_g(\mathbf{x})}{\frac{1}{2}[p_r(\mathbf{x}) + p_g(\mathbf{x})]} - 2 \cdot \log 2. \end{aligned} \quad (3)$$

Equation 3 demonstrates the loss function for a GAN when discriminator is optimized and it is related to two important probability measurement metrics. One is Kullback–Leibler (KL) divergence which is defined as

$$KL(p_1 \| p_2) = \mathbb{E}_{\mathbf{x} \sim p_1} \log \frac{p_1}{p_2}, \quad (4)$$

and the other is Jensen-Shannon (JS) divergence which is stated as

$$\begin{aligned} JS(p_1 \| p_2) &= \frac{1}{2} KL(p_1 \| \frac{p_1 + p_2}{2}) + \\ &\quad \frac{1}{2} KL(p_2 \| \frac{p_1 + p_2}{2}). \end{aligned} \quad (5)$$

Thus the loss for  $G$  regarding the optimal  $D$  in equation (3) can be reformulated as

$$\mathcal{L}_G = 2 \cdot JS(p_r \| p_g) - 2 \cdot \log 2, \quad (6)$$

which indicates that the loss for  $G$  now equally becomes the minimization of the JS divergence between  $p_r$  and  $p_g$ . With the training  $D$  step by step, the optimization of  $G$  will be closer to the minimization of JS divergence between  $p_r$  and  $p_g$ . We now start to explain the unstable training problem, where  $D$  often easily wins  $G$ . This unstable training problem is actually caused by the JS divergence in equation (5). Give an optimal  $D$ , the objective of optimization for equation (6) is to move  $p_g$  toward  $p_r$  (see Fig. 9). JS divergence for the three plots from left to right are 0.693, 0.693 and 0.336, which indicates that JS divergence stay constant ( $\log 2 = 0.693$ ) if there is no overlap between  $p_r$  and  $p_g$ . Figure 10 demonstrates the change of JS divergence and its gradient corresponding to the distance between  $p_r$  and  $p_g$ . It can be seen that JS divergence is constant and its gradient is almost 0 when the distance is greater than 5, which indicates that training process does not have any effect on  $G$ . The gradient of JS divergence for training the  $G$  is non-zero only when  $p_g$  and  $p_r$  have non-ignorable overlap i.e. the vanishing gradient will arise for  $G$  when  $D$  is close to optimal. In reality, the possibility that  $p_r$  and  $p_g$  does not overlap or have ignorable overlap is very high [86].

Original work [1] also states minimizing  $-\mathbb{E}_{\mathbf{x} \sim p_g} \log[D(\mathbf{x})]$  for training  $G$  to avoid the vanishing gradient as stated before. However, this training strategy

will lead to another problem called mode dropping. First, let us look at the  $KL(p_g \| p_r) = \mathbb{E}_{\mathbf{x} \sim p_g} \log \frac{p_g}{p_r}$ . With an optimal discriminator  $D^*$ ,  $KL(p_g \| p_r)$  can be reformulated as

$$\begin{aligned} KL(p_g \| p_r) &= \mathbb{E}_{\mathbf{x} \sim p_g} \log \frac{p_g(\mathbf{x})/(p_r(\mathbf{x}) + p_g(\mathbf{x}))}{p_r(\mathbf{x})/(p_r(\mathbf{x}) + p_g(\mathbf{x}))}, \\ &= \mathbb{E}_{\mathbf{x} \sim p_g} \log \frac{1 - D^*(\mathbf{x})}{D^*(\mathbf{x})}, \\ &= \mathbb{E}_{\mathbf{x} \sim p_g} \log[1 - D^*(\mathbf{x})] - \\ &\quad \mathbb{E}_{\mathbf{x} \sim p_g} \log[D^*(\mathbf{x})]. \end{aligned} \quad (7)$$

The alternative loss for  $G$  now can be stated by switching the order the two sides in equation (7)

$$\begin{aligned} & - \mathbb{E}_{\mathbf{x} \sim p_g} \log[D^*(\mathbf{x})] \\ &= KL(p_g \| p_r) - \mathbb{E}_{\mathbf{x} \sim p_g} \log[1 - D^*(\mathbf{x})], \\ &= KL(p_g \| p_r) - 2 \cdot JS(p_r \| p_g) + \\ &\quad 2 \log 2 + \mathbb{E}_{\mathbf{x} \sim p_r} \log[D^*(\mathbf{x})], \end{aligned} \quad (8)$$

where the alternative loss for  $G$  in equation (8) is only affected by the first two terms (last two terms are constant). It can be noticed that the optimization in equation (8) is contradictory because the first term aims to push the generated distribution toward the real distribution while the second term aim to push in the opposite direction (the negative sign). This will cause unstable numerical gradient for training  $G$ . More importantly, KL divergence is unsymmetrical distribution measurement where is highlighted below

- When  $p_g(\mathbf{x}) \rightarrow 0, p_r(\mathbf{x}) \rightarrow 1, KL(p_g \| p_r) \rightarrow 0$ .
- When  $p_g(\mathbf{x}) \rightarrow 1, p_r(\mathbf{x}) \rightarrow 0, KL(p_g \| p_r) \rightarrow +\infty$ .

The penalization for two mistakes made by  $G$  are totally different. The first mistake is that  $G$  does not produce very plausible samples and it has very tiny penalization. The second mistake is that  $G$  produce implausible samples but it has very large penalization. The first mistake is that generated samples lack the diversity while the second mistake is the generated samples are not accurate. Considering this case,  $G$  prefers to generating repeated but “safe” samples instead of taking risk to generate diverse but “unsafe” samples, which leads to the mode collapse problem. In summary, using the original loss in equation (1) will get the vanishing gradient for training  $G$  and using the alternative loss in equation (8) will have the mode collapse problem. These kind of problems cannot be solved by changing the architectures for GANs. Therefore, the ultimate problem of GANs is caused the loss function and the hard core techniques for re-designing the loss function will completely solve the problem.

Loss-variant GANs have been researched extensively to improve the stability of training GANs.

## 6.1 Wasserstein GAN (WGAN)

WGAN [87] has successfully solved the two problems for the original GAN by using the Earth mover (EM) or Wasserstein-1 [88] distance as the loss for optimization. The EM distance is defined as

$$W(p_r, p_g) = \inf_{\gamma \in \Pi(p_r, p_g)} \mathbb{E}_{(\mathbf{x}, \mathbf{y}) \sim \gamma} \|\mathbf{x} - \mathbf{y}\|, \quad (9)$$

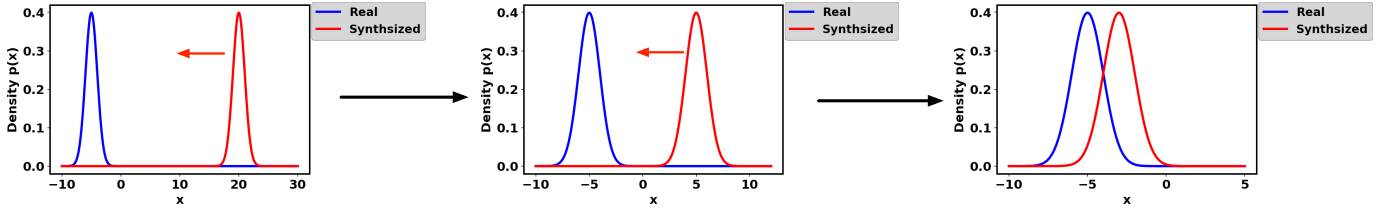
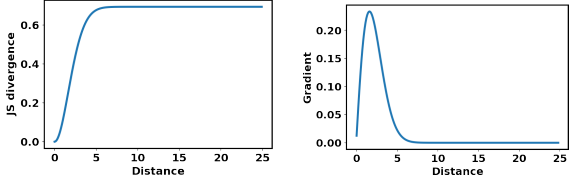


Fig. 9. Explanation training progress for a GAN. Two normal distributions are used here for visualization. Given an optimal  $D$ , the objective of GANs is to update  $G$  in order to move the generated distribution  $p_g$  (red) towards the real distribution  $p_r$  (blue) ( $G$  supposes to be updated as seen from left to right). Left: initial state, middle: during training, right: training converging). However, JS divergence for left two figures are both 0.693 and right figure is 0.336, which indicates that JS divergence cannot provide sufficient gradient at the initial state.



(a) JS divergence changes with distance. (b) Gradient JS divergence changes with distance.

Fig. 10. JS divergence and gradient change with the distance between  $p_r$  and  $p_g$ . The distance is the difference between two distribution means.

where  $\prod(p_r, p_g)$  denotes the set of all joint distributions and  $\gamma(x, y)$  whose marginals are  $p_r$  and  $p_g$ . Comparing to KL divergence and JS divergence, EM is able to reflect the distance even  $p_r$  and  $p_g$  are not overlapped and it is also continuous which is able to provide meaningful gradient for training the generator. Figure. 18 illustrates the gradient of WGAN comparing to the original GAN. It can be noticed that WGAN has the smooth gradient for training generator spanning all space. Wasserstein distance has much nicer properties comparing to JS divergence. However, the infimum in equation (9) is intractable. Author demonstrates that Wasserstein distance can be estimated as

$$\max_{w \sim \mathcal{W}} \mathbb{E}_{\mathbf{x}_{p_r}} [f_w(\mathbf{x})] - \mathbb{E}_{\mathbf{z} \sim p_z} [f_w(G(\mathbf{z}))], \quad (10)$$

where  $f_w$  can be realized by  $D$  but has some constrains (details can refer to the original work [87]) and  $\mathbf{z}$  is the input noise for  $G$ . So  $w$  here is the parameters in  $D$  and  $D$  aims to maximize equation (10) in order to make the optimization distance equivalent to Wasserstein distance. When  $D$  is optimized, equation (9) will become the Wasserstein distance and  $G$  aims to minimize it. So the loss for  $G$  is

$$- \min_G \mathbb{E}_{\mathbf{z} \sim p_z} [f_w(G(\mathbf{z}))] \quad (11)$$

An important difference between WGAN and original GAN is the function of  $D$ . The  $D$  in original work is used as a binary classifier but  $D$  used in WGAN is to fit the Wasserstein distance, which is a regression task. Thus, the sigmoid in the last layer of  $D$  is removed in the WGAN.

## 6.2 WGAN-GP

Even WGAN has successfully improved the stability of training GANs, it is not well generalized for a deeper model. Experiment finds that most parameters of WGAN

are localized at -0.01 and 0.01 because of the parameter clipping. This will dramatically reduce the modeling capacity for  $D$ . WGAN-GP is proposed using gradient penalty for restricting  $\|f\|_L \leq K$  for discriminator [55] and the modified loss for discriminator now becomes

$$\mathcal{L}_D = \mathbb{E}_{\mathbf{x}_g \sim p_g} [D(\mathbf{x}_g)] - \mathbb{E}_{\mathbf{x}_r \sim p_r} [D(\mathbf{x}_r)] + \lambda \mathbb{E}_{\hat{\mathbf{x}} \sim p_{\hat{x}}} [(\|\nabla_{\hat{\mathbf{x}}} D(\hat{\mathbf{x}})\|_2 - 1)^2], \quad (12)$$

where  $\mathbf{x}_r$  is sample data drawn from real data distribution  $p_r$ ,  $\mathbf{x}_g$  is sample data drawn from generated data distribution  $p_g$  and  $p_{\hat{x}}$  sampling uniformly along the straight lines between pairs of points sampled from the real data distribution  $p_r$  and generated data distribution  $p_g$ , first two terms are original critic loss in WGAN and the last term is the gradient penalty. WGAN-GP shows a better distribution of trained parameters comparing to WGAN (Fig. 11) and better stability performance during training GANs.

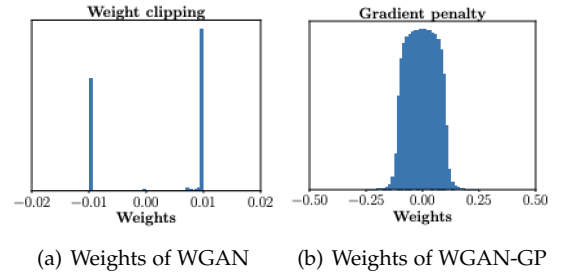


Fig. 11. Comparison of parameter distribution between WGAN and WGAN-GP. Top is WGAN and bottom is WGAN-GP. Figure from [55].

## 6.3 Least Square GAN (LSGAN)

LSGAN is proposed in [89] to remedy the vanishing gradient problem for  $G$  from the perspective of decision boundary which is made by discriminator. This work argues that the decision boundary for  $D$  of original GAN penalizes the tiny error to update  $G$  for those generated samples are far away from the decision boundary. Author proposes using least square loss for  $D$  instead of sigmoid cross entropy loss stated in the original paper [1]. The proposed loss function is defined as

$$\begin{aligned} \min_D \mathcal{L}_D &= \frac{1}{2} \mathbb{E}_{\mathbf{x} \sim p_r} [(D(\mathbf{x}) - b)^2] + \\ &\quad \frac{1}{2} \mathbb{E}_{\mathbf{z} \sim p_z} [(D(G(\mathbf{z})) - a)^2], \quad (13) \\ \min_G \mathcal{L}_G &= \frac{1}{2} \mathbb{E}_{\mathbf{z} \sim p_z} [(D(G(\mathbf{z})) - c)^2], \end{aligned}$$

where  $a$  is the label for generated samples,  $b$  is the label for real sample and  $c$  is the value that  $G$  wants  $D$  to believe for generated samples. This modified change has two benefits: (1) The new decision boundary made by  $D$  penalizes large error to those generated samples that is far away from the decision boundary, which pushes those "bad" generated samples moving toward the decision boundary. This is beneficial to generating good image quality; (2) Penalizing the generated samples far away from the decision boundary can provide more gradient when updating the  $G$ , which remedies the vanishing gradient problems for training  $G$ . Figure. 12 demonstrates the comparison of decision boundaries for LSGAN and original GAN. The decision boundaries for  $D$  that trained by original sigmoid cross entropy loss and the proposed least square loss are different. More importantly, errors of the "bad" generated samples (in magenta) are penalized differently by original GAN and LSGAN, which can refers the two loss functions for  $G$ . The work [89] has proven that the optimization of LSGAN is equivalent to minimizing the Pearson  $\chi^2$  divergence between  $p_r + p_g$  and  $2p_g$  when  $a, b$  and  $c$  satisfy the condition of  $b - c = 1$  and  $b - a = 2$ . Similar to WGAN,  $D$  here behaves as regression and the sigmoid is also removed.

#### 6.4 f-GAN

f-GAN summarizes that GANs can be trained by using any f-divergence [90]. f-divergence is a function  $D_f(P||Q)$  that measures the difference between probability distribution  $P$  and  $Q$ . e.g., KL divergence, JS divergence and Pearson  $\chi^2$  as mentioned before. This work discusses the efficacy of various divergence function in terms of training complexity and the quality of the generative models.

#### 6.5 Unrolled GAN (UGAN)

UGAN is proposed to solve the mode collapse for GANs during the training [91]. The core design of UGAN is adding a gradient term for updating  $G$  that captures how the discriminator would react to a change in the generator. The optimal parameter of  $D$  can be expressed as the fixed point of an iterative optimization procedure

$$\begin{aligned} \theta_D^0 &= \theta_D, \\ \theta_D^{k+1} &= \theta_D^k + \eta^k \frac{df(\theta_G, \theta_D^k)}{d\theta_D^k}, \\ \theta_D^*(\theta_G) &= \lim_{k \rightarrow \infty} \theta_D^k, \end{aligned} \quad (14)$$

where  $\eta^k$  is the learning rate,  $\theta_D$  represents parameters for  $D$  and  $\theta_G$  represents parameters for  $G$ . The surrogate loss by unrolling for  $K$  steps can be expressed as

$$f_K(\theta_G, \theta_D) = f(\theta_G, \theta_D^K(\theta_G, \theta_D)). \quad (15)$$

This surrogate loss is then used for updating parameters for  $D$  and  $G$

$$\begin{aligned} \theta_G &\leftarrow \theta_G - \eta \frac{df_K(\theta_G, \theta_D)}{d\theta_G}, \\ \theta_D &\leftarrow \theta_D + \eta \frac{df(\theta_G, \theta_D)}{d\theta_D} \end{aligned} \quad (16)$$

Figure. 13 illustrates the computation graph for an unrolled

GAN with 3 unrolling steps. Equation (17) illustrates the gradient for updating  $G$ .

$$\begin{aligned} \frac{df_K(\theta_G, \theta_D)}{d\theta_G} &= \frac{\partial f(\theta_G, \theta_D^K(\theta_G, \theta_D))}{\theta_G} + \\ &\frac{\partial f(\theta_G, \theta_D^K(\theta_G, \theta_D))}{\partial \theta_D^K(\theta_G, \theta_D)} \frac{d\theta_D^K(\theta_G, \theta_D)}{d\theta_G} \end{aligned} \quad (17)$$

It should be noted that the first term in equation (17) is the gradient for the original GAN. The second term here reflects that how  $D$  reacts to the change in the  $G$ . If  $G$  tends to collapse to one mode,  $D$  will increase the loss for  $G$ . Thus, this unrolled approach is able to prevent the mode collapse problem for GANs.

#### 6.6 Loss Sensitive GAN (LS-GAN)

LS-GAN is introduced to train a generator to produce realistic samples by minimizing the designated margins between real and generated samples [92]. This work argues that the problems such as vanishing gradient and model collapse appearing in the original GAN is caused by a non-parametric hypothesis that the discriminator is able to distinguish any type of probability distribution between real samples and generated samples. As mentioned before, it is very normal for the overlap between real samples distribution and the generated samples distribution are ignorable. Moreover,  $D$  is also able to separate real samples and generated samples. The JS divergence will become a constant under this situation, where the vanishing gradient arises for  $G$ . In LS-GAN, the classification ability of  $D$  is restricted and is learned by a loss function  $L_\theta(\mathbf{x})$  parameterized with  $\theta$ , which assumed that a real sample ought to have smaller loss than a generated sample. The loss function can be trained as the following constraint:

$$L_\theta(\mathbf{x}) \leq L_\theta(G(\mathbf{z})) - \Delta(\mathbf{x}, G(\mathbf{z})), \quad (18)$$

where  $\Delta(\mathbf{x}, G(\mathbf{z}))$  is the margin measuring the difference between real samples and generated samples. This constraint indicates that a real sample is separated from a generated sample by at least a margin of  $\Delta(\mathbf{x}, G(\mathbf{z}))$ . The optimization for LS-GAN is stated as

$$\begin{aligned} \min_D \mathcal{L}_D &= \mathbb{E}_{\mathbf{x} \sim p_r} L_\theta(\mathbf{x}) + \\ &\lambda \mathbb{E}_{\substack{\mathbf{x} \sim p_r \\ \mathbf{z} \sim p_z}} (\Delta(\mathbf{x}, G(\mathbf{z})) + \\ &L_\theta(\mathbf{x}) - L_\theta(G(\mathbf{z})))_+, \\ \min_G \mathcal{L}_G &= \mathbb{E}_{\mathbf{z} \sim p_z} L_\theta(G(\mathbf{z})), \end{aligned} \quad (19)$$

where  $\lambda$  is a positive balancing parameter,  $(a)_+ = \max(a, 0)$  and  $\theta$  is the parameters in  $D$ . From the second term in  $\mathcal{L}_D$  in the equation (19),  $\Delta(\mathbf{x}, G(\mathbf{z}))$  is added as a regularizer term for optimizing  $D$  in order to prevent  $D$  from perfectly separating the real samples and the generated samples. Figure. 14 demonstrates the efficacy of the equation (19). Loss for  $D$  puts the restriction on the ability of  $D$  i.e. It challenges the ability of  $D$  for well separation between generated samples and real samples, which is the original cause for the vanishing gradient. LS-GAN assumes that  $p_r$  lies in a set of Lipschitz densities with a compact support.



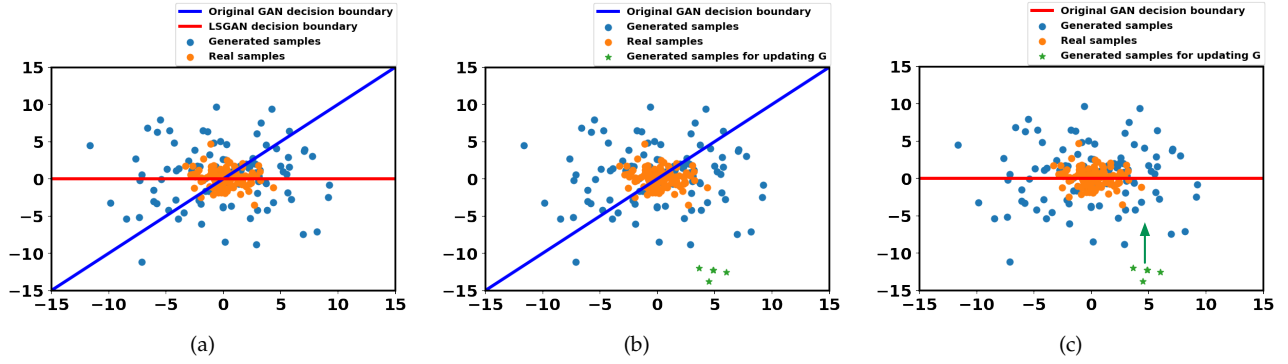


Fig. 12. Decision boundary illustration of original GAN and LSGAN. (a). Decision boundaries for  $D$  of original GAN and LSGAN. (b). Decision boundary of  $D$  for the original GAN. It gets small errors for the generated samples, which is far away from the decision boundary (in green), for updating  $G$ . (c). Decision boundary for  $D$  of LSGAN. It penalizes the large error for generated sample that is far away from the boundary (in green). Thus it pushes generated samples (in green) toward the boundary [89].

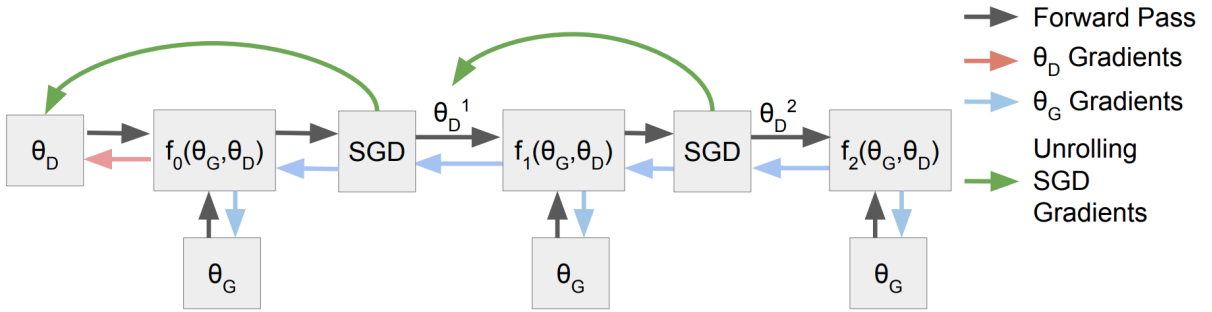


Fig. 13. An example of computation for an unrolled GAN with 3 unrolling steps.  $G$  and  $D$  update using equation (16). Each step  $k$  uses the gradients of  $f_k$  regarding  $\theta_D^k$  stated in the equation (14) [91].

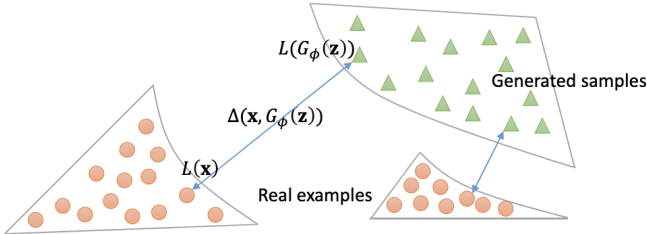


Fig. 14. Demonstration of the loss in equation (19).  $\Delta(\mathbf{x}, G(\mathbf{z}))$  is used to separate real samples and generated samples. If some generated samples are close to real samples enough, LS-GAN will work focus on other generated samples that are far away from the real samples. This optimization loss puts restriction on  $D$  to prevent it from separating generated and real samples perfectly. Thus, it solves the vanishing gradient problem arises in original GAN. ( $G_\phi(\mathbf{z})$  here is equivalent to  $G(\mathbf{z})$  where  $\phi$  represents the parameters for generator) [92].

## 6.7 Mode Regularized GAN (MRGAN)

MRGAN proposes the metric regularizer to penalize missing modes [93], which is used to solve the mode collapse problem. The key idea of this work is using an encoder  $E(\mathbf{x})$ :  $\mathbf{x} \rightarrow \mathbf{z}$  to produce the latent variable  $\mathbf{z}$  for  $G$  instead of using noise. This procedure has two benefits: (1) The reconstruction of encoder can add more information to  $G$

so it is not that easy for  $D$  distinguish between generated samples and real samples; and (2) Encoder guarantees the correspondence between  $\mathbf{x}$  and  $\mathbf{z}$  ( $E(\mathbf{x})$ ), which makes  $G$  able to cover different modes in the  $\mathbf{x}$  space. So it prevents the mode collapse problem. The loss function for Mode regularized GAN is

$$\begin{aligned} \mathcal{L}_G &= -\mathbb{E}_{\mathbf{z}}[\log[D(G(\mathbf{z}))]] + \\ &\quad \mathbb{E}_{\mathbf{x} \sim p_r}[\lambda_1 d(\mathbf{x}, G \circ E(\mathbf{x})) + \\ &\quad \lambda_2 \log[D(G(\mathbf{x}))]], \end{aligned} \quad (20)$$

$$\mathcal{L}_E = \mathbb{E}_{\mathbf{x} \sim p_r}[\lambda_1 d(\mathbf{x}, G \circ E(\mathbf{x})) + \lambda_2 \log[D(G(\mathbf{x}))]],$$

where  $d$  is a geometric measurement which can be chose in many options e.g., pixel-wise  $L^2$  and distance of extracted features.

## 6.8 Geometric GAN

Geometric GAN [94] is proposed using SVM separating hyperplane, which has the maximal margins between the two classes. Figure. 15 demonstrates the updating rule for discriminator and generator based on the SVM hyperplane. Geometric GAN has been successfully demonstrated that is more stable for training and less mode collapsing.

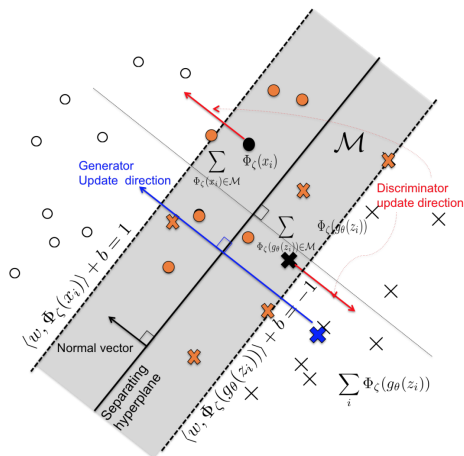


Fig. 15. SVM hyperplane used in Geometric GAN. Discriminator updates by pushing real data samples and generated data samples away from the hyperplane while generator updates by pushing generated data samples towards the hyperplane. Figure from [94].

## 6.9 Relativistic GAN (RGAN)

RGAN [95] is proposed as a general approach in devising new cost functions from the existing one i.e. it can be generalized for all integral probability metric (IPM) [96], [97] GANs. The discriminator in original GAN measures *how real the probability is for a given real sample or a generated sample*. Author argues that a key relative discriminant information is missing from standard GANs. Discriminator in RGAN takes account that *how given a real sample is more realistic than a randomly sampled generated sample*. Loss function of RGAN applied to original GAN is stated as

$$\begin{aligned} & \min_D \mathbb{E}_{\mathbf{x}_r \sim p_r} \mathbb{E}_{\mathbf{x}_g \sim p_g} [\log(\text{sigmoid}(C(\mathbf{x}_r) - C(\mathbf{x}_g)))] \\ & \min_G \mathbb{E}_{\mathbf{x}_r \sim p_r} \mathbb{E}_{\mathbf{x}_g \sim p_g} [\log(\text{sigmoid}(C(\mathbf{x}_g) - C(\mathbf{x}_r)))] \end{aligned} \quad (21)$$

where  $C(\mathbf{x})$  is the non-transformed layer. Figure. 16 demon-

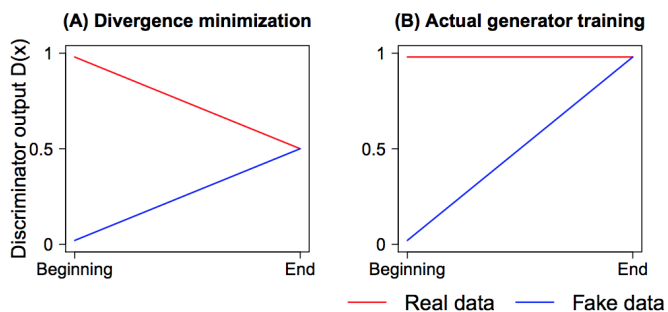


Fig. 16.  $D$  output comparison between RGAN and original GAN. (a)  $D$  output in RGAN; (b)  $D$  output in original GAN when training the  $G$ . Figure from [95].

strates the efficacy on  $D$  by using RGAN comparing to the original GAN. In terms of the original GAN, the optimization aims to push the  $D(\mathbf{x})$  to 1 (right one). For RGAN, the optimization aims to push  $D(\mathbf{x})$  to 0.5 (left one), which is

more stable comparing to the original GAN. Author also claims that RGAN can be generalized to other types of loss-variant GANs if those loss functions belong to IPMs. The generalization loss is stated as

$$\begin{aligned} \mathcal{L}_D &= \mathbb{E}_{\mathbf{x}_r \sim p_r} [f_1(C(x_r) - C(x_g))] + \\ & \mathbb{E}_{\mathbf{x}_g \sim p_g} [f_2(C(x_g) - C(x_r))], \\ \mathcal{L}_G &= \mathbb{E}_{\mathbf{x}_r \sim p_r} [g_1(C(x_r) - C(x_g))] + \\ & \mathbb{E}_{\mathbf{x}_g \sim p_g} [g_2(C(x_g) - C(x_r))], \end{aligned} \quad (22)$$

where  $f_1(y) = g_2(y) = -y$  and  $f_2(y) = g_1(y) = y$ . Details of loss generalization for other GANs refers to the original paper [95].

## 6.10 Spectral normalization GAN (SN-GAN)

SN-GAN is proposed by using weight normalization to stabilize the training of discriminator. This technique is computationally light and easily applied to existing GANs. Previous work for stabilizing the training GANs [55], [87], [92] explain the importance that  $D$  is from the set of  $K$ -Lipshitz continuous function. Popularly speaking, Lipschitz continuous [98]–[100] is more strict than the continuous, which describes that the function does not change rapidly. This smooth  $D$  is of benefit to stabilize training the GANs. The work mentioned before focus on the control of the Lipschitz constant of the discriminator function. This work demonstrates a simple way to control the Lipschitz constant by spectral normalizing each layer for  $D$ . Spectral normalization is done as

$$\bar{\mathbf{W}}_{SN}(\mathbf{W}) = \frac{\mathbf{W}}{\sigma(\mathbf{W})}, \quad (23)$$

where  $\mathbf{W}$  represents weights on each layer for  $D$  and  $\sigma(\mathbf{W})$  is  $L_2$  matrix norm of  $\mathbf{W}$ . Paper proves this will make  $\|f\| \leq 1$ . The fast approximation for the  $\sigma(\mathbf{W})$  is also demonstrated in the original paper.

## 6.11 Summary

We explain the training problems (mode collapse and vanishing gradient for  $G$ ) in the original GAN and we have introduced loss-variant GANs in the literature, which are mainly proposed for improving the performance for GANs from three aspects. Figure. 17 summarizes the efficacy of loss-variant GANs for the challenges. Losses of LSGAN, RGAN and WGAN are very similar to the original GAN loss. We use a toy example (i.e., two distributions used in Fig. 9) to demonstrate the  $G$  loss regarding the distance between real data distribution and generated data distribution in Fig. 18. It can be seen that RGAN and WGAN are able to inherently solve the vanishing gradient problems for generator when discriminator is optimized. LSGAN on the contrary still suffers vanishing gradient for generator, however, it is able to provide more sufficient gradient comparing to original GAN in Fig. 10 when the distance between real data distribution and generated data distribution is relatively small. This is demonstrated in the original paper [89] that LSGAN is easier to push generated sample to the boundary.

Table 1 gives detail illustration on the properties of each

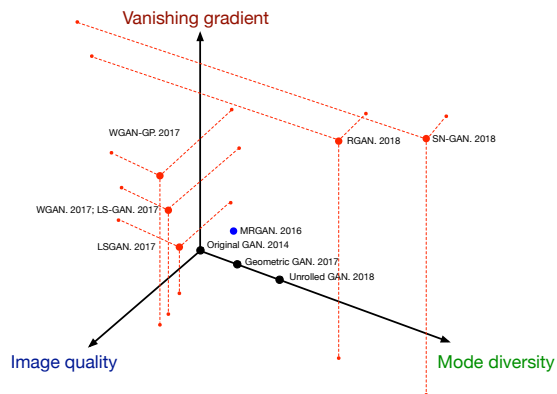


Fig. 17. Current loss-variants for solving the challenges. Challenges are categorized by three orthogonal axes. Red points indicate the GAN-variant covers all three challenges, blue points cover two, and black points cover only one challenge. Larger value for each axis indicates better performance.

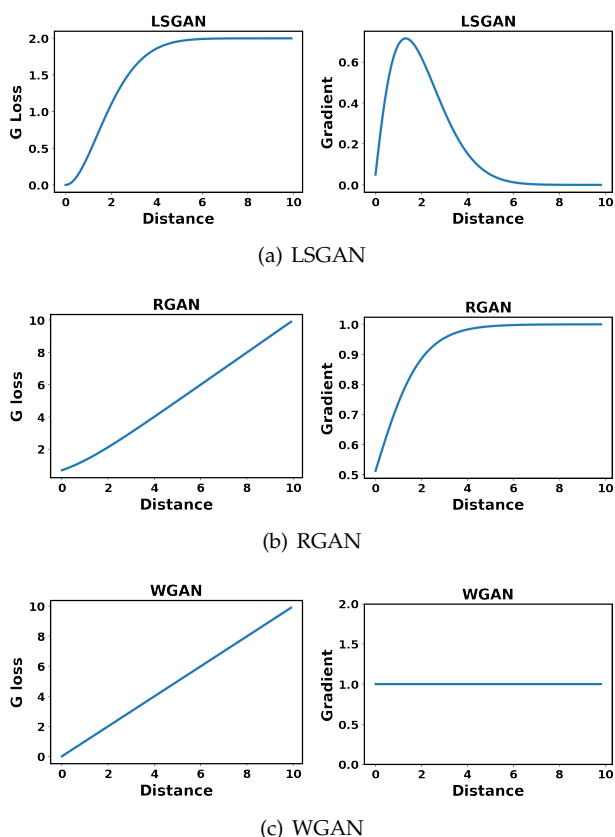


Fig. 18. Loss and gradient for generator of different loss-variant GANs.

loss-variant GAN. WGAN, LSGAN, LS-GAN, RGAN and SN-GAN are proposed to overcome the vanishing gradient for  $G$ . LSGAN argues that the vanishing gradient is mainly caused by the sigmoid function in the discriminator so it uses the least square loss to optimize the GAN. LSGAN turns out the optimization on Pearson  $\chi^2$  divergence and it successfully solves the vanishing gradient problem. WGAN uses Wasserstein (or Earth mover) distance as the loss. Comparing to JS divergence, Wasserstein distance is smoother and there is no sudden change. To be able to use Wasserstein distance as the loss, discriminator has to be restricted to

Lipschitz continuous, where WGAN deploys the parameter clipping to force discriminator satisfy the Lipschitz continuous. However, it causes problems such as most of parameters in the discriminator locates to the edges of clipping range, which leads to the low capacity of discriminator. WGAN-GP is proposed the use of gradient penalty to make discriminator is Lipschitz continuous, which successfully solves the problems in WGAN. LS-GAN proposes to use a margin that is enforced to separate real samples from generated samples, which restricts the modelling capability of discriminator. It solves the vanishing gradient for generator because this problem arises when discriminator is optimized. RGAN is a unified framework that is suitable for all IPM-based GAN e.g., WGAN. RGAN adds the discriminant information to GAN for better learning. SN-GAN proposes an elegant way for optimizing a GAN. As mentioned before, Lipschitz continuous for discriminator is important for stable learning, vanishing gradient and so on. SN-GAN proposes spectral normalization [66] to restrict discriminator under the Lipschitz continuous requirement. SN-GAN is the first GAN (we do not consider AC-GANs [11] because an ensemble of 100 AC-GANs is used for Imagenet datasets [101].) that has been successfully applied to Imagenet datasets. In theory, spectral normalization in SN-GAN is able to applied for each type of GANs. SAGAN and BigGAN [83], [85] both deploy the spectral normalization and achieve good results in the Imagenet.

Loss-variant GANs are well-generalized to architecture-variants. However, SN-GAN and RGAN show the stronger generalization ability comparing to other loss-variants, where these two loss-variants can be generalized to other types of loss-variants. Spectral normalization is able to be generalized to any type of GAN variant while RGAN can be generalized to any IPM-based GAN. We strongly recommend the use of spectral normalization for each type of GAN. There are some other loss-variant GANs mentioned in this paper in order to solve the mode collapse and unstable training problem. Details can refer to Table 1.

## 7 DISCUSSION

We have introduced the inherent problems in the original GAN which are mode collapse and vanishing gradient for updating  $G$ . We have surveyed some GAN-variants that remedy these problems from two aspects: (1) Architecture-variant. This aspect focuses on revising architectures for GAN. This approach enables GANs successfully being applied for different applications, however, it is not able to fully solve the problems mentioned above; (2) Loss-variant. We have provided a detail explanation why these problems arise in the original GAN. These problems are essentially caused by the loss function in the original GAN. Thus, modifying loss function for GANs would be the ultimate solution. It should be noted that the loss function may be changed as well for some architecture-variant GANs. However, this loss function is revised by changing the architecture which is architecture-specific loss. It is not able to generalize to other architectures.

By comparing the different architectures in this work, it can be noticed that the modification of the architecture for GANs has the impact on the generated image quality

and diversity. Recent research shows that the capacity and performance of GANs are related to the architecture size and batch size [83], which indicates that a proper architecture is critical to a GAN. However, modification on architecture only is not able to eliminate the inherent training problems for GANs. Redesign of loss function including regularization and normalization can help more stable training for GANs. This work introduced various ways of designing the loss function for GANs. Based on the comparison for each loss-variant, we find spectral normalization in SN-GAN favors lots of benefits including easy to implement, light computation and able to generalize to almost each type of GANs. We suggest researchers who apply GANs to real-world application to include the spectral normalization to the discriminator.

There is no answer to define which GAN is best. The selection of GAN-variant depends on different applications. For instance, if there is an application requiring that produce natural scenes images (this requires generated images are very diverse). DCGAN with spectrum normalization applied, SAGAN and BigGAN can be good choice. BigGAN is able to produce the most realistic images comparing to other two. However, BigGAN costs much more computation resource. Thus it depends on the actual requirements asked by real-world applications.

### 7.1 Interconnections Between Architecture and Loss

In this paper, we explain the inherent problems in the original GAN. By remedying those problems, we study architecture-variants and loss-variants of GANs separately. However, it should be noted that there are interconnections between these two types of GAN variants. As mentioned before, loss functions are easily integrated to different architectures. Benefit from good convergence and stabilization of redesigned loss, architecture-variants are able to achieve better performance and accomplish more difficult problems. For examples, BEGAN and PROGAN use Wasserstein distance instead of JS divergence. SAGAN and BigGAN deploy the spectral normalization, where they achieve good performance based on multi-class image generation. These two types of variants equally contribute to the progress of GANs.

### 7.2 Future Directions

GANs are originally proposed in order to produce plausible images and have achieved exciting performance in computer vision area. GANs have been applied to some other fields, (e.g., time series generation [20], [21], [102] and natural language processing [15], [103]–[105]). Comparing to computer vision, GANs research in other areas is still limited. The limitation is caused by the different properties between image and non-image data. For instance, GANs work to produce the continuous value data but natural language are based on discrete values like words, characters, bytes, etc., so it is hard to apply GANs for natural language applications. Future research can be carried out for applying GANs for other areas.

## 8 CONCLUSION

In this paper, we review the GAN-variants based on performance improvement including high image quality, more diverse images and stable training. We review the current GAN-related research from architecture and loss basis. Current state-of-arts GAN models such as BigGAN and PROGAN. are able to produce high quality images and diverse images in the computer vision field. However, research that applies GANs to video is limited. Moreover, GANs-related research in other areas such as time series generation and natural language processing fall behind the computer vision area a lot. Future research for GANs can be carried out in those fields.

### ACKNOWLEDGMENT

This work is funded as part of the Insight Centre for Data Analytics which is supported by Science Foundation Ireland under Grant Number SFI/12/RC/2289. The authors would like to thank the blogs posted on Zhihu, Quora, Medium etc., which provide the informative insight on the GANs-related research.

### REFERENCES

- [1] I. Goodfellow, J. Pouget-Abadie, M. Mirza, B. Xu, D. Warde-Farley, S. Ozair, A. Courville, and Y. Bengio, "Generative adversarial nets," in *Advances in Neural Information Processing Systems*, 2014, pp. 2672–2680.
- [2] M.-Y. Liu and O. Tuzel, "Coupled generative adversarial networks," in *Advances in neural information processing systems*, 2016, pp. 469–477.
- [3] T. Salimans, I. Goodfellow, W. Zaremba, V. Cheung, A. Radford, and X. Chen, "Improved techniques for training GANs," in *Advances in Neural Information Processing Systems*, 2016, pp. 2234–2242.
- [4] M. O. Turkoglu, L. Spreeuwens, W. Thong, and B. Kicanaoglu, "A layer-based sequential framework for scene generation with GANs," in *Thirty-Third AAAI Conference on Artificial Intelligence*, Honolulu, Hawaii, United States, 2019.
- [5] H. Wu, S. Zheng, J. Zhang, and K. Huang, "GP-GAN: Towards realistic high-resolution image blending," *arXiv preprint arXiv:1703.07195*, 2017.
- [6] J. Pan, C. C. Ferrer, K. McGuinness, N. E. O'Connor, J. Torres, E. Sayrol, and X. Giro-i Nieto, "SalGAN: Visual saliency prediction with generative adversarial networks," *arXiv preprint arXiv:1701.01081*, 2017.
- [7] G. K. Dziugaite, D. M. Roy, and Z. Ghahramani, "Training generative neural networks via maximum mean discrepancy optimization," *arXiv preprint arXiv:1505.03906*, 2015.
- [8] L. Ma, X. Jia, Q. Sun, B. Schiele, T. Tuytelaars, and L. Van Gool, "Pose guided person image generation," in *Advances in Neural Information Processing Systems*, 2017, pp. 406–416.
- [9] C. Vondrick, H. Pirsaviash, and A. Torralba, "Generating videos with scene dynamics," in *Advances In Neural Information Processing Systems*, 2016, pp. 613–621.
- [10] C. Yang, X. Lu, Z. Lin, E. Shechtman, O. Wang, and H. Li, "High-resolution image inpainting using multi-scale neural patch synthesis," in *Proceedings of the IEEE Conference on Computer Vision and Pattern Recognition*, 2017, pp. 6721–6729.
- [11] A. Odena, C. Olah, and J. Shlens, "Conditional image synthesis with auxiliary classifier gans," in *Proceedings of the 34th International Conference on Machine Learning*, vol. 70. JMLR, 2017, pp. 2642–2651.
- [12] Y. Li, K. Swersky, and R. Zemel, "Generative moment matching networks," in *International Conference on Machine Learning*, 2015, pp. 1718–1727.
- [13] J.-Y. Zhu, P. Krähenbühl, E. Shechtman, and A. A. Efros, "Generative visual manipulation on the natural image manifold," in *European Conference on Computer Vision*. Springer, 2016, pp. 597–613.

- [14] C. Lassner, G. Pons-Moll, and P. V. Gehler, "A generative model of people in clothing," in *Proceedings of the IEEE International Conference on Computer Vision*, 2017, pp. 853–862.
- [15] W. Fedus, I. Goodfellow, and A. M. Dai, "MaskGAN: Better text generation via filling in the \_," *arXiv preprint arXiv:1801.07736*, 2018.
- [16] Z. Yang, J. Hu, R. Salakhutdinov, and W. Cohen, "Semi-supervised QA with generative domain-adaptive nets," in *Proceedings of the 55th Annual Meeting of the Association for Computational Linguistics (Volume 1: Long Papers)*, Vancouver, Canada, 2017, pp. 1040–1050.
- [17] Z. Dai, Z. Yang, F. Yang, W. W. Cohen, and R. R. Salakhutdinov, "Good semi-supervised learning that requires a bad GAN," in *Advances in neural information processing systems*, 2017, pp. 6510–6520.
- [18] N. Jetchev, U. Bergmann, and R. Vollgraf, "Texture synthesis with spatial generative adversarial networks," *arXiv preprint arXiv:1611.08207*, 2016.
- [19] C. Donahue, J. McAuley, and M. Puckette, "Synthesizing audio with generative adversarial networks," *arXiv preprint arXiv:1802.04208*, 2018.
- [20] K. G. Hartmann, R. T. Schirrmeyer, and T. Ball, "EEG-GAN: Generative adversarial networks for electroencephalographic brain signals," *arXiv preprint arXiv:1806.01875*, 2018.
- [21] C. Esteban, S. L. Hyland, and G. Rätsch, "Real-valued (medical) time series generation with recurrent conditional GANs," *arXiv preprint arXiv:1706.02633*, 2017.
- [22] D. Li, D. Chen, L. Shi, B. Jin, J. Goh, and S.-K. Ng, "MAD-GAN: Multivariate anomaly detection for time series data with generative adversarial networks," *arXiv preprint arXiv:1901.04997*, 2019.
- [23] W. Zhu, X. Xiang, T. D. Tran, and X. Xie, "Adversarial deep structural networks for mammographic mass segmentation," *arXiv preprint arXiv:1612.05970*, 2016.
- [24] P. Luc, C. Couprie, S. Chintala, and J. Verbeek, "Semantic segmentation using adversarial networks," *arXiv preprint arXiv:1611.08408*, 2016.
- [25] H. Dong, S. Yu, C. Wu, and Y. Guo, "Semantic image synthesis via adversarial learning," in *Proceedings of the IEEE International Conference on Computer Vision*, 2017, pp. 5706–5714.
- [26] Z. Qiu, Y. Pan, T. Yao, and T. Mei, "Deep semantic hashing with generative adversarial networks," in *Proceedings of the 40th International ACM SIGIR Conference on Research and Development in Information Retrieval*. ACM, 2017, pp. 225–234.
- [27] N. Souly, C. Spampinato, and M. Shah, "Semi supervised semantic segmentation using generative adversarial network," in *Proceedings of the IEEE International Conference on Computer Vision*, 2017, pp. 5688–5696.
- [28] T. Karras, S. Laine, and T. Aila, "A style-based generator architecture for generative adversarial networks," *arXiv preprint arXiv:1812.04948*, 2018.
- [29] T.-C. Wang, M.-Y. Liu, J.-Y. Zhu, A. Tao, J. Kautz, and B. Catanzaro, "High-resolution image synthesis and semantic manipulation with conditional GANs," in *Proceedings of the IEEE Conference on Computer Vision and Pattern Recognition*, 2018, pp. 8798–8807.
- [30] B. Poole, A. A. Alemi, J. Sohl-Dickstein, and A. Angelova, "Improved generator objectives for GANs," *arXiv preprint arXiv:1612.02780*, 2016.
- [31] J. Choe, S. Park, K. Kim, J. Hyun Park, D. Kim, and H. Shim, "Face generation for low-shot learning using generative adversarial networks," in *Proceedings of the IEEE International Conference on Computer Vision*, 2017, pp. 1940–1948.
- [32] H. Zhang, T. Xu, H. Li, S. Zhang, X. Wang, X. Huang, and D. N. Metaxas, "Stackgan: Text to photo-realistic image synthesis with stacked generative adversarial networks," in *Proceedings of the IEEE International Conference on Computer Vision*, 2017, pp. 5907–5915.
- [33] J.-Y. Zhu, T. Park, P. Isola, and A. A. Efros, "Unpaired image-to-image translation using cycle-consistent adversarial networks," *arXiv preprint arXiv:1703.10593v6*, 2017.
- [34] J.-Y. Zhu, R. Zhang, D. Pathak, T. Darrell, A. A. Efros, O. Wang, and E. Shechtman, "Toward multimodal image-to-image translation," in *Advances in Neural Information Processing Systems*, 2017, pp. 465–476.
- [35] M. Tomei, M. Cornia, L. Baraldi, and R. Cucchiara, "Art2Real: Unfolding the reality of artworks via semantically-aware image-to-image translation," *arXiv preprint arXiv:1811.10666*, 2018.
- [36] M.-Y. Liu, T. Breuel, and J. Kautz, "Unsupervised image-to-image translation networks," in *Advances in Neural Information Processing Systems*, 2017, pp. 700–708.
- [37] P. Isola, J.-Y. Zhu, T. Zhou, and A. A. Efros, "Image-to-image translation with conditional adversarial networks," in *Proceedings of the IEEE conference on computer vision and pattern recognition*, 2017, pp. 1125–1134.
- [38] Y. Choi, M. Choi, M. Kim, J.-W. Ha, S. Kim, and J. Choo, "StarGAN: Unified generative adversarial networks for multi-domain image-to-image translation," in *Proceedings of the IEEE Conference on Computer Vision and Pattern Recognition*, 2018, pp. 8789–8797.
- [39] S. Ma, J. Fu, C. Wen Chen, and T. Mei, "DA-GAN: Instance-level image translation by deep attention generative adversarial networks," in *Proceedings of the IEEE Conference on Computer Vision and Pattern Recognition*, 2018, pp. 5657–5666.
- [40] C. Ledig, L. Theis, F. Huszár, J. Caballero, A. Cunningham, A. Acosta, A. Aitken, A. Tejani, J. Totz, Z. Wang et al., "Photo-realistic single image super-resolution using a generative adversarial network," in *2017 IEEE Conference on Computer Vision and Pattern Recognition*. IEEE, 2017, pp. 105–114.
- [41] X. Wang, K. Yu, S. Wu, J. Gu, Y. Liu, C. Dong, Y. Qiao, and C. Change Loy, "ESRGAN: Enhanced super-resolution generative adversarial networks," in *European Conference on Computer Vision Workshop*, 2018.
- [42] D. Mahapatra, B. Bozorgtabar, S. Hewavitharanage, and R. Garnavi, "Image super resolution using generative adversarial networks and local saliency maps for retinal image analysis," in *International Conference on Medical Image Computing and Computer-Assisted Intervention*. Springer, 2017, pp. 382–390.
- [43] D. Mahapatra, B. Bozorgtabar, and R. Garnavi, "Image super-resolution using progressive generative adversarial networks for medical image analysis," *Computerized Medical Imaging and Graphics*, vol. 71, pp. 30–39, 2019.
- [44] J. Yu, Z. Lin, J. Yang, X. Shen, X. Lu, and T. S. Huang, "Generative image inpainting with contextual attention," *arXiv preprint arXiv:1801.07892*, 2018.
- [45] R. A. Yeh, C. Chen, T. Yian Lim, A. G. Schwing, M. Hasegawa-Johnson, and M. N. Do, "Semantic image inpainting with deep generative models," in *Proceedings of the IEEE Conference on Computer Vision and Pattern Recognition*, 2017, pp. 5485–5493.
- [46] B. Dolhansky and C. Canton Ferrer, "Eye in-painting with exemplar generative adversarial networks," in *Proceedings of the IEEE Conference on Computer Vision and Pattern Recognition*, 2018, pp. 7902–7911.
- [47] Z. Chen, S. Nie, T. Wu, and C. G. Healey, "High resolution face completion with multiple controllable attributes via fully end-to-end progressive generative adversarial networks," *arXiv preprint arXiv:1801.07632*, 2018.
- [48] Y. Li, S. Liu, J. Yang, and M.-H. Yang, "Generative face completion," in *Proceedings of the IEEE Conference on Computer Vision and Pattern Recognition*, 2017, pp. 3911–3919.
- [49] J. Kossaiji, L. Tran, Y. Panagakis, and M. Pantic, "GANGAN: Geometry-aware generative adversarial networks," in *Proceedings of the IEEE Conference on Computer Vision and Pattern Recognition*, 2018, pp. 878–887.
- [50] Q. Dai, Q. Li, J. Tang, and D. Wang, "Adversarial network embedding," in *Thirty-Second AAAI Conference on Artificial Intelligence*, 2018.
- [51] N. Kodali, J. Abernethy, J. Hays, and Z. Kira, "On convergence and stability of gans," *arXiv preprint arXiv:1705.07215*, 2017.
- [52] Y. Li, A. Schwing, K.-C. Wang, and R. Zemel, "Dualizing GANs," in *Advances in Neural Information Processing Systems*, 2017, pp. 5606–5616.
- [53] A. Borji, "Pros and cons of GAN evaluation measures," *Computer Vision and Image Understanding*, vol. 179, pp. 41–65, 2019.
- [54] Q. Xu, G. Huang, Y. Yuan, C. Guo, Y. Sun, F. Wu, and K. Weinberger, "An empirical study on evaluation metrics of generative adversarial networks," *arXiv preprint arXiv:1806.07755*, 2018.
- [55] I. Gulrajani, F. Ahmed, M. Arjovsky, V. Dumoulin, and A. C. Courville, "Improved training of wasserstein GANs," in *Advances in Neural Information Processing Systems*, 2017, pp. 5767–5777.
- [56] M. Heusel, H. Ramsauer, T. Unterthiner, B. Nessler, and S. Hochreiter, "GANs trained by a two time-scale update rule converge to a local nash equilibrium," in *Advances in Neural Information Processing Systems*, 2017, pp. 6626–6637.

- [57] A. Gretton, K. M. Borgwardt, M. J. Rasch, B. Schölkopf, and A. Smola, "A kernel two-sample test," *Journal of Machine Learning Research*, vol. 13, no. Mar, pp. 723–773, 2012.
- [58] Z. Wang, G. Healy, A. F. Smeaton, and T. E. Ward, "Use of neural signals to evaluate the quality of generative adversarial network performance in facial image generation," *arXiv preprint arXiv:1811.04172*, Submitted to *Cognitive Computation*, March, 2019.
- [59] Z. Wang, Q. She, A. F. Smeaton, T. E. Ward, and G. Healy, "Neuroscore: A brain-inspired evaluation metric for generative adversarial networks," *arXiv preprint arXiv:1905.04243*, 2019.
- [60] S. Barratt and R. Sharma, "A note on the inception score," *arXiv preprint arXiv:1801.01973*, 2018.
- [61] L. Theis, A. v. d. Oord, and M. Bethge, "A note on the evaluation of generative models," *arXiv preprint arXiv:1511.01844*, 2015.
- [62] K. Kurach, M. Lucic, X. Zhai, M. Michalski, and S. Gelly, "The GAN landscape: Losses, architectures, regularization, and normalization," *arXiv preprint arXiv:1807.04720*, 2018.
- [63] F. Yu, A. Seff, Y. Zhang, S. Song, T. Funkhouser, and J. Xiao, "Lsun: Construction of a large-scale image dataset using deep learning with humans in the loop," *arXiv preprint arXiv:1506.03365*, 2015.
- [64] Z. Liu, P. Luo, X. Wang, and X. Tang, "Large-scale celebfaces attributes (celeba) dataset," *Retrieved August*, vol. 15, p. 2018, 2018.
- [65] A. Krizhevsky and G. Hinton, "Learning multiple layers of features from tiny images," Citeseer, Tech. Rep., 2009.
- [66] Y. Yoshida and T. Miyato, "Spectral norm regularization for improving the generalizability of deep learning," *arXiv preprint arXiv:1705.10941*, 2017.
- [67] S. Hitawala, "Comparative study on generative adversarial networks," *arXiv preprint arXiv:1801.04271*, 2018.
- [68] K. Wang, C. Gou, Y. Duan, Y. Lin, X. Zheng, and F.-Y. Wang, "Generative adversarial networks: introduction and outlook," *IEEE/CAA Journal of Automatica Sinica*, vol. 4, no. 4, pp. 588–598, 2017.
- [69] A. Creswell, T. White, V. Dumoulin, K. Arulkumaran, B. Sengupta, and A. A. Bharath, "Generative adversarial networks: An overview," *IEEE Signal Processing Magazine*, vol. 35, no. 1, pp. 53–65, 2018.
- [70] Y. Hong, U. Hwang, J. Yoo, and S. Yoon, "How generative adversarial networks and their variants work: An overview," *ACM Computing Surveys (CSUR)*, vol. 52, no. 1, p. 10, 2019.
- [71] A. Radford, L. Metz, and S. Chintala, "Unsupervised representation learning with deep convolutional generative adversarial networks," *arXiv preprint arXiv:1511.06434*, 2015.
- [72] D. Berthelot, T. Schumm, and L. Metz, "BEGAN: Boundary equilibrium generative adversarial networks," *arXiv preprint arXiv:1703.10717*, 2017.
- [73] T. Karras, T. Aila, S. Laine, and J. Lehtinen, "Progressive growing of gans for improved quality, stability, and variation," *arXiv preprint arXiv:1710.10196*, 2017.
- [74] S. Iizuka, E. Simo-Serra, and H. Ishikawa, "Globally and locally consistent image completion," *ACM Transactions on Graphics (ToG)*, vol. 36, no. 4, p. 107, 2017.
- [75] S. Reed, Z. Akata, X. Yan, L. Logeswaran, B. Schiele, and H. Lee, "Generative adversarial text to image synthesis," *arXiv preprint arXiv:1605.05396*, 2016.
- [76] Y. LeCun, L. Bottou, Y. Bengio, P. Haffner *et al.*, "Gradient-based learning applied to document recognition," *Proceedings of the IEEE*, vol. 86, no. 11, pp. 2278–2324, 1998.
- [77] E. L. Denton, S. Chintala, R. Fergus *et al.*, "Deep generative image models using a laplacian pyramid of adversarial networks," in *Advances in neural information processing systems*, 2015, pp. 1486–1494.
- [78] M. Mirza and S. Osindero, "Conditional generative adversarial nets," *arXiv preprint arXiv:1411.1784*, 2014.
- [79] P. Burt and E. Adelson, "The Laplacian pyramid as a compact image code," *IEEE Transactions on communications*, vol. 31, no. 4, pp. 532–540, 1983.
- [80] M. D. Zeiler and R. Fergus, "Visualizing and understanding convolutional networks," in *European conference on computer vision*. Springer, 2014, pp. 818–833.
- [81] J. Zhao, M. Mathieu, and Y. LeCun, "Energy-based generative adversarial network," *arXiv preprint arXiv:1609.03126*, 2016.
- [82] A. A. Rusu, N. C. Rabinowitz, G. Desjardins, H. Soyer, J. Kirkpatrick, K. Kavukcuoglu, R. Pascanu, and R. Hadsell, "Progressive neural networks," *arXiv preprint arXiv:1606.04671*, 2016.
- [83] A. Brock, J. Donahue, and K. Simonyan, "Large scale GAN training for high fidelity natural image synthesis," *arXiv preprint arXiv:1809.11096*, 2018.
- [84] A. Vaswani, N. Shazeer, N. Parmar, J. Uszkoreit, L. Jones, A. N. Gomez, Ł. Kaiser, and I. Polosukhin, "Attention is all you need," in *Advances in Neural Information Processing Systems*, 2017, pp. 5998–6008.
- [85] H. Zhang, I. Goodfellow, D. Metaxas, and A. Odena, "Self-attention generative adversarial networks," *arXiv preprint arXiv:1805.08318*, 2018.
- [86] M. Arjovsky and L. Bottou, "Towards principled methods for training generative adversarial networks," *arXiv preprint arXiv:1701.04862*, 2017.
- [87] M. Arjovsky, S. Chintala, and L. Bottou, "Wasserstein GAN," *arXiv preprint arXiv:1701.07875*, 2017.
- [88] Y. Rubner, C. Tomasi, and L. J. Guibas, "The earth mover's distance as a metric for image retrieval," *International journal of computer vision*, vol. 40, no. 2, pp. 99–121, 2000.
- [89] X. Mao, Q. Li, H. Xie, R. Y. Lau, Z. Wang, and S. P. Smolley, "Least squares generative adversarial networks," in *2017 IEEE International Conference on Computer Vision*. IEEE, 2017, pp. 2813–2821.
- [90] S. Nowozin, B. Cseke, and R. Tomioka, "f-GAN: Training generative neural samplers using variational divergence minimization," in *Advances in neural information processing systems*, 2016, pp. 271–279.
- [91] L. Metz, B. Poole, D. Pfau, and J. Sohl-Dickstein, "Unrolled generative adversarial networks," *arXiv preprint arXiv:1611.02163*, 2016.
- [92] G.-J. Qi, "Loss-sensitive generative adversarial networks on lipschitz densities," *arXiv preprint arXiv:1701.06264*, 2017.
- [93] T. Che, Y. Li, A. P. Jacob, Y. Bengio, and W. Li, "Mode regularized generative adversarial networks," *arXiv preprint arXiv:1612.02136*, 2016.
- [94] J. H. Lim and J. C. Ye, "Geometric GAN," *arXiv preprint arXiv:1705.02894*, 2017.
- [95] A. Jolicoeur-Martineau, "The relativistic discriminator: a key element missing from standard GAN," *arXiv preprint arXiv:1807.00734*, 2018.
- [96] B. K. Sriperumbudur, K. Fukumizu, A. Gretton, B. Schölkopf, and G. R. Lanckriet, "On integral probability metrics,  $\phi$ -divergences and binary classification," *arXiv preprint arXiv:0901.2698*, 2009.
- [97] A. Müller, "Integral probability metrics and their generating classes of functions," *Advances in Applied Probability*, vol. 29, no. 2, pp. 429–443, 1997.
- [98] T. Donchev and E. Farkhi, "Stability and euler approximation of one-sided lipschitz differential inclusions," *SIAM journal on control and optimization*, vol. 36, no. 2, pp. 780–796, 1998.
- [99] L. Armijo, "Minimization of functions having lipschitz continuous first partial derivatives," *Pacific Journal of mathematics*, vol. 16, no. 1, pp. 1–3, 1966.
- [100] A. Goldstein, "Optimization of lipschitz continuous functions," *Mathematical Programming*, vol. 13, no. 1, pp. 14–22, 1977.
- [101] J. Deng, W. Dong, R. Socher, L.-J. Li, K. Li, and L. Fei-Fei, "Imagenet: A large-scale hierarchical image database," in *2009 IEEE conference on computer vision and pattern recognition*. IEEE, 2009, pp. 248–255.
- [102] Y. Luo, X. Cai, Y. Zhang, J. Xu *et al.*, "Multivariate time series imputation with generative adversarial networks," in *Advances in Neural Information Processing Systems*, 2018, pp. 1596–1607.
- [103] L. Yu, W. Zhang, J. Wang, and Y. Yu, "SeqGAN: Sequence generative adversarial nets with policy gradient," in *Thirty-First AAAI Conference on Artificial Intelligence*, 2017.
- [104] D. Bahdanau, P. Brakel, K. Xu, A. Goyal, R. Lowe, J. Pineau, A. Courville, and Y. Bengio, "An actor-critic algorithm for sequence prediction," *arXiv preprint arXiv:1607.07086*, 2016.
- [105] J. Li, W. Monroe, A. Ritter, M. Galley, J. Gao, and D. Jurafsky, "Deep reinforcement learning for dialogue generation," *arXiv preprint arXiv:1606.01541*, 2016.

TABLE 1  
Summary of loss-variant for GANs.

Author & Year	GAN type	Pros	Cons
Goodfellow et al. 2014	Original GAN	<ol style="list-style-type: none"> <li>1. Generate samples very fast.</li> <li>2. Able to deal with sharp probability distribution.</li> </ol>	<ol style="list-style-type: none"> <li>1. Vanishing gradient for <math>G</math>.</li> <li>2. Mode collapse.</li> <li>3. Resolution of generated images is very low.</li> </ol>
Chen et al. 2016	MORGAN	<ol style="list-style-type: none"> <li>1. Improve the mode diversity.</li> <li>2. Stabilize the training for the GAN.</li> </ol>	<ol style="list-style-type: none"> <li>1. Generated image quality is low.</li> <li>2. Have not solved vanishing gradient problem for <math>G</math>.</li> <li>3. Only tested on CelebA dataset. Have not tested on more diverse image datasets e.g., CIFAR and ImageNet.</li> </ol>
Nowozin et al. 2016	f-GAN	<ol style="list-style-type: none"> <li>1. Provide a unified framework based on f-divergence.</li> </ol>	<ol style="list-style-type: none"> <li>1. Have not specified the stability for different f-divergence functions.</li> <li>1. Large weight clipping causes long time to converge and small weight clipping causes vanishing gradient.</li> <li>2. Weight clipping reduces the capacity of the model and limits the capability to model complex function.</li> <li>3. Very deep WGAN is hard to converge.</li> </ol>
Arjovsky et al. 2017	WGAN	<ol style="list-style-type: none"> <li>1. Solve the vanishing gradient problem.</li> <li>2. Improve the image quality.</li> <li>3. Solve the mode collapse.</li> </ol>	<ol style="list-style-type: none"> <li>1. Cannot use batch normalization because gradient penalization is done for each sample in the batch.</li> </ol>
Gulrajani et al. 2017	WGAN-GP	<ol style="list-style-type: none"> <li>1. Converges much faster than WGAN.</li> <li>2. Model is more stable during the training.</li> <li>3. Able to use deeper GAN to model more complex function.</li> </ol>	<ol style="list-style-type: none"> <li>1. Generated samples are pushed to decision boundary instead of real data, which may affect the generated image quality.</li> </ol>
Mao et al. 2017	LSGAN	<ol style="list-style-type: none"> <li>1. Remedy the vanishing gradient and stabilized the training for GANs.</li> <li>2. Improve the mode diversity for model.</li> <li>3. Easy to implement.</li> </ol>	<ol style="list-style-type: none"> <li>1. Difficult to implement. Lots of tiny pieces have to be carefully designed for loss function.</li> <li>2. The margin added between real samples and generated samples may affect the quality of generated images.</li> </ol>
Qi. 2017	LS-GAN	<ol style="list-style-type: none"> <li>1. Solve the vanishing gradient problem.</li> <li>2. Solve the mode collapse problem.</li> </ol>	<ol style="list-style-type: none"> <li>1. Have not demonstrated the ability against the vanishing gradient.</li> <li>2. Experiment tests have to be done on more complex datasets e.g., ImageNet.</li> </ol>
Lim et al. 2017	Geometric GAN	<ol style="list-style-type: none"> <li>1. Less mode collapsing.</li> <li>2. More stable for training.</li> <li>3. Converges to the Nash equilibrium between the discriminator and generator.</li> </ol>	<ol style="list-style-type: none"> <li>1. The quality of generated image is low.</li> </ol>
Metz et al. 2018	Unrolled GAN	<ol style="list-style-type: none"> <li>1. Solve the mode collapse problem.</li> <li>2. Demonstrate that high order gradient information can help train a GAN.</li> <li>3. Improve the training stability for GAN.</li> </ol>	<ol style="list-style-type: none"> <li>1. Lack of mathematical implications of adding relativism to GANs.</li> <li>2. Have not done a survey which IPM-based GAN will achieve the best performance with being added the relativism.</li> </ol>
Martineau. 2018	RGAN	<ol style="list-style-type: none"> <li>1. Solve the vanishing gradient problem.</li> <li>2. Unified framework for IPM-based GANs.</li> <li>3. Solve the mode collapse problems.</li> </ol>	<ol style="list-style-type: none"> <li>1. Need to test on more complex image datasets.</li> </ol>
Miyato et al. 2018	SN-GAN	<ol style="list-style-type: none"> <li>1. Computationally light and easy to implement on existing GANs.</li> <li>2. Improve the image quality and solve the mode collapse.</li> <li>3. Stabilize the training GANs and solve the vanishing gradient problem.</li> </ol>	

## SUPPLEMENTARY MATERIAL

Details of searched papers are included in Fig. 19 and Fig. 20. Figure 19 illustrates the number of papers in each

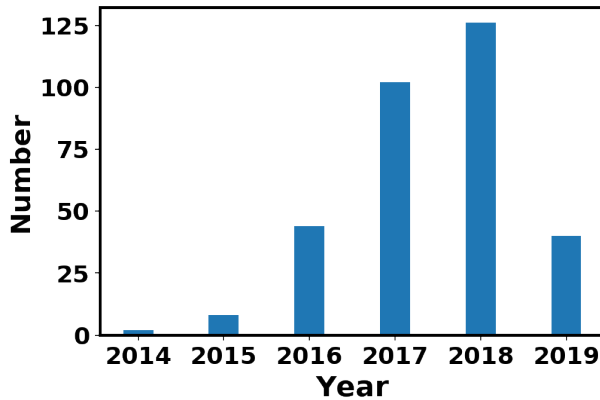


Fig. 19. Number of papers in each year from 2014 to 17th May 2019.

year from 2014 to 2019. It can be seen that the number of papers increases each year from 2014 to 2018. As our search ends up on 17th May 2019, this number can not represent the overall number of papers in 2019. Especially there are several upcoming top-tier conferences e.g., CVPR, ICCV, NeurIPS, and ICML, where much more papers may come out later this year. Even given this situation, the number of papers in 2019 is close to that in 2016. It can be noticed that there is significant rise of papers in 2016 and 2017. Indeed we see lots of exciting research in these two years e.g., CoGAN, f-GAN in 2016 and WGAN, PROGAN in 2017, which pushes the GANs research and exposes GANs to the public. In 2018, GANs still attracts lots of attention and the number of papers is more than that in previous years.

Figure 20 illustrates the number of papers published on

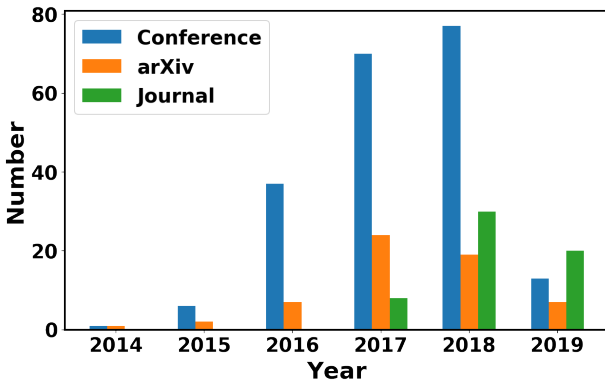


Fig. 20. Categories of papers from 2014 to 17th May 2019. Papers are categorized as conference, arXiv and journal.

three repositories, namely conference, arXiv and journal. Conference takes the largest amount from 2015 to 2018 and dramatic increase appears in 2016 and 2017. As mentioned before, there are several top-tier upcoming conferences later this year, conference supposes to take the lead on the number of papers in 2019. Papers published on Journal starts to increase since from 2017, which may be caused by the reviewing duration for a journal paper is longer

than a conference paper and of course much longer than an arXiv paper. As GANs are well-developed and well-known to researchers from different areas today, number of journal papers related to GANs supposes to maintain the increasing tendency in 2019. It is interesting that number of arXiv pre-prints reaches the peak in 2017 and then starts to descend. We guess this is caused by more and more papers are accepted by conference and journal so arXiv pre-prints claim the publication details, which leads to the decreasing number of pre-prints on arXiv. This indicates higher quality of GANs research in recent years from the other side. Figure 21 gives an illustration on the percentage

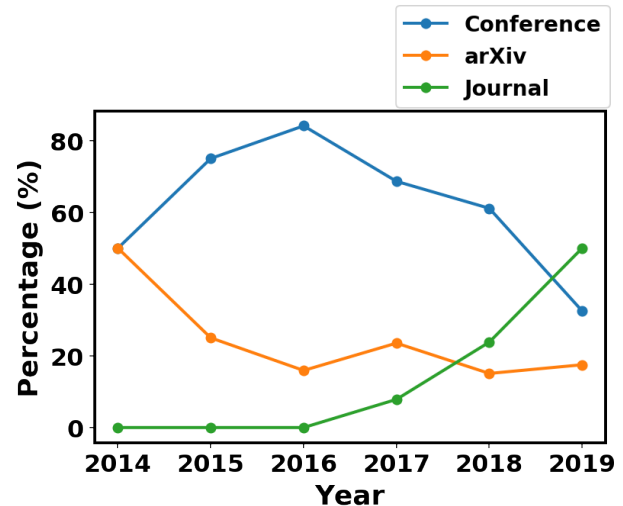


Fig. 21. Percentages of each category take account the total number of papers in each year.

of each category taking account the total number of papers in each year. Supporting results in Fig. 20, tendency of number of journal papers keeps going up. Percentage of number of conference papers reaches peak at 2016 then begins to descend. It should be noted that this does not mean the decrease of number of conference papers. This is due to other categories (i.e., arXiv and journal papers) start to increase.

A detail of searched papers are listed on this link: <https://cutt.ly/GAN-CV-paper>.